

## Understanding Scuffing and Micropitting of Gears

R W Snidle, H P Evans, M P Alanou, M J A Holmes

School of Engineering  
Cardiff University  
Cardiff CF24 0YF, UK

[SnidleR@cf.ac.uk](mailto:SnidleR@cf.ac.uk)

### ABSTRACT

*The paper describes the results of basic research, both theoretical and experimental, on scuffing and micropitting of gears used in naval and aerospace applications. Scuffing experiments have been carried out under severe conditions of load, sliding speed and temperature using typical gear steels with different surface treatments including case-carburising, nitriding, superfinishing, and super-hard coatings. The results of this work demonstrate the importance of surface finish not only in improving scuffing resistance, but also in reducing contact friction and energy losses. Theoretical work on microelastohydrodynamic lubrication shows the importance of surface roughness in terms of high pressures generated at surface asperities on gear teeth and the effect this has upon the distribution of stress very close to the tooth surface. Some new microelastohydrodynamic parameters, derived from this work, are of potential use in discriminating between different types of gear finishes in terms of their tendency to generate extremes of pressure and film thinning which are of direct relevance to micropitting.*

### 1.0 INTRODUCTION

Gears transmit power through rolling/sliding contacts between their teeth, which must operate reliably for many thousands of hours with negligible wear. Lubrication of tooth contacts, both as a means of minimising surface damage and as a way of reducing friction due to sliding, is therefore of crucial importance. Gears have been made from various materials, including polymers, but in this paper we are concerned with steel gears which are the most important type in use in vehicles, aerospace, marine and industrial applications. It is now known that elastohydrodynamic lubrication (EHL) is the mechanism responsible for the protection of steel gear teeth. The basic kinematics of involute gears (by far the most important type) necessitate a relatively low geometrical conformity between the mating teeth (Figure 1) and this gives rise to contact pressures, which can be as high as 1.5 GPa if high strength surface-hardened steels are used. Under these conditions the viscosity of typical lubricating oils is increased by several orders of magnitude and significant “Hertzian” elastic deformation of the surfaces occurs. Sliding also takes place between the teeth given by

$$u_s = (\omega_1 + \omega_2)s$$

where  $s$  is the distance of the instantaneous contact between the teeth from the pitch point  $Z$  shown in Figure 1 and  $\omega_1$  and  $\omega_2$  are the angular velocities of the two gears. The entraining velocity, which is responsible for the formation of any oil film by hydrodynamic action, is given by

$$\bar{u} = (r_{b1} \tan \psi + s)\omega_1 / 2 + (r_{b2} \tan \psi - s)\omega_2 / 2$$

Both sliding and entraining velocities therefore vary throughout the meshing cycle as does the relative contact geometry. A typical ratio of the sliding to entraining velocities at the extremes of tooth contact is

*Paper presented at the RTO AVT Specialists' Meeting on “The Control and Reduction of Wear in Military Platforms”, held in Williamsburg, USA, 7-9 June 2003, and published in RTO-MP-AVT-109.*

## Understanding Scuffing and Micropitting of Gears

about 0.5, but can be as high as unity in very coarse gears. Contact loads are uncertain due to load-sharing between simultaneous, overlapping tooth contacts, and dynamic effects at high speeds. A necessary compromise in high speed gear design is the need to minimise sliding by using rather small teeth whilst choosing teeth of sufficient size to resist the bending stresses caused by tooth loading. This explains the use of rather fine pitch teeth combined with relatively large face-width in high speed naval reduction units.

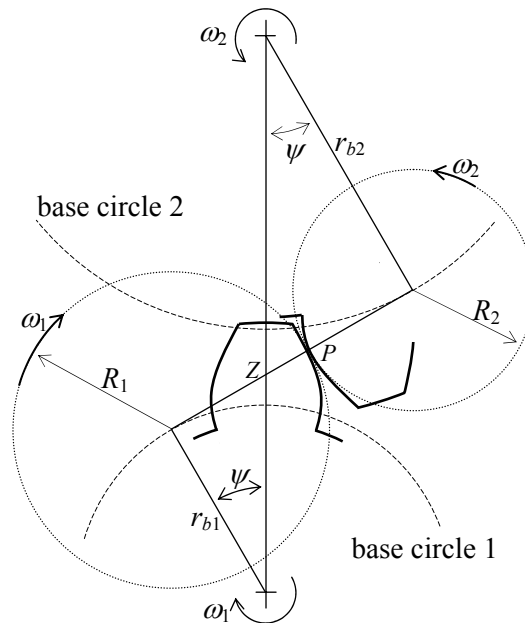


**Figure 1: Illustration of gear teeth in contact showing equivalent rolling/sliding circles. Sliding is proportional to  $s = ZP$ , where  $Z$  is the pitch point and  $P$  is the instantaneous contact between the teeth.**

Lubricant film thickness in involute gear teeth is usually assessed using EHL line contact theory [1] in the form of Dowson and Higginson's formula

$$h_{\min}/R = 1.6(\alpha)^{0.6}(\eta_0 \bar{u})^{0.7}(E')^{0.03}R^{-0.57}w'^{-0.13}$$

which has been experimentally validated for smooth surfaces, most notably by Dyson et al [2]. Modifications are available for situations where the underlying assumptions do not apply, e.g. to correct for temperature rise in the inlet to the contact [3]. This theory is for infinitely long "line" contacts which is the situation in the majority of both spur and helical involute gears. Gears that have "point" contacts such as those in "Wildhaber-Novikov" [4] conformal gears, and angle-drive gears such as hypoids and spiral bevels, require formulas for predicting film thickness under side-leakage conditions [5,6].

Under ideal conditions gear teeth operate with films which effectively separate the surfaces, and the above EHL film formula may be used. However, under demanding conditions of low speed or high temperature, the film predicted by classical EHL theory may be small compared with the roughness present on the teeth. The gears then operate under conditions described as "partial", "mixed" or "micro" EHL. A conventional measure of the severity of lubrication is provided by the lambda-ratio, which is defined as the mean oil film thickness divided by the combined RMS roughness of the two surfaces, i.e.

$$\Lambda = h/\sqrt{\sigma_1^2 + \sigma_2^2}$$

Parameter  $\Lambda$  has been used as an indicator of relative life in rolling element bearings [7]. Most gears, however, are much rougher than bearings and rarely have a finish better than about  $0.4 \mu\text{m } R_a$  with

nominal oil films typically 1  $\mu\text{m}$  at most. Clearly, many practical gears operate with  $\lambda$  significantly less than unity. In theoretical solutions of both the dry contact and micro-EHL problems significant roughness leads to a severe rippling in the contact pressure distribution with maximum values far in excess of the Hertzian values for smooth surfaces. Surface roughness effects are important in the gearing problems of "micropitting" and "scuffing" [8] which are discussed in Sections 2 and 3.

This paper briefly reviews some current research on gear tooth contact lubrication that will lead to a better understanding of the problems of micropitting, scuffing and gear and transmission lubrication in general.

## 2.0 MICROPITTING

Micropitting is pitting (rolling contact fatigue) on the scale of the roughness, as opposed to classical pitting which occurs on the scale of the nominal Hertzian, or macro, contact. With increased use of hardened gears it has become of widespread concern to the gearing industry. Although it can affect all types of gears, it has become particularly troublesome in heavily loaded gears with hardened teeth. The problem has been extensively studied by researchers [9,10,11,12] and is well known to gear designers [13]. Micropitting is characterised by the presence of fine surface pits and the occurrence of local plastic deformation and shallow surface cracks. It produces significant wear of the surfaces causing loss of profile of the teeth, leading to noise. Serious cases can precipitate scuffing and even complete fracture of the tooth. The problem is widespread and its solution has a high industrial priority. Figure 2 shows a gear tooth with characteristic micropitting damage.

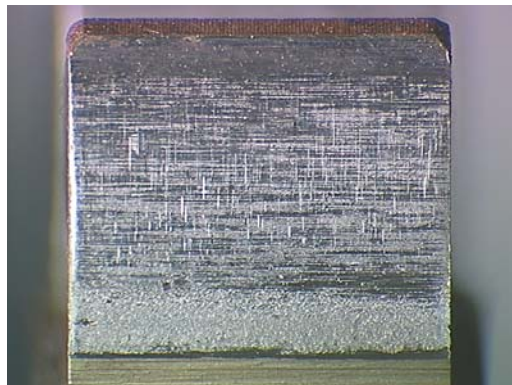


**Figure 2: Gear tooth showing micropitting damage in the root region. (Design Unit, Newcastle University)**

The causes of micropitting are not fully understood, but surface roughness and high contact stresses at asperity or micro contacts within the overall Hertzian contact are key features, so that a thorough understanding of the stresses at asperity contacts is clearly needed. Useful insights into the behaviour of the contact of real surfaces can be obtained using dry elastic contact simulations [14,15] or elastic/plastic contact simulations [16]. However, it is necessary to consider the micro-EHL effects of the oil film since these influence the contact pressures and, through non-Newtonian and time-dependent behaviour, determine the traction forces at the micro contacts. The important sub-surface stress field is therefore affected by the presence of a micro EHL film. In general when roughness is present the maximum sub-surface shear stress field occurs much closer to the surface as seen in the micro EHL simulations in section 4.

The mechanism of plastic ratchetting brought about by asperity pummelling or cyclic stressing at the edges of micro contacts described by Kapoor and Johnson [17] may also be a factor in micropitting, and work directed towards an understanding of failure of railway wheel contacts undergoing plastic

## Understanding Scuffing and Micropitting of Gears

deformation may also be relevant [18]. Cavitation occurring within the nominal EHL contact due to asperity action discussed in Section 4 may also be a factor contributing to micropitting.

Recent fatigue testing of gears in the ground and superfinished state [19] shows the benefit to be obtained in terms of pitting life by superfinishing. Figure 3 is a Weibull plot comparing performance of hardened, ground steel gears (mean  $R_a = 0.38 \mu\text{m}$ ) with superfinished gears (mean  $R_a = 0.07 \mu\text{m}$ ) of the same material. The lives of the gears with superfinished teeth in this programme were found to be about four times greater than those of the ground gears.

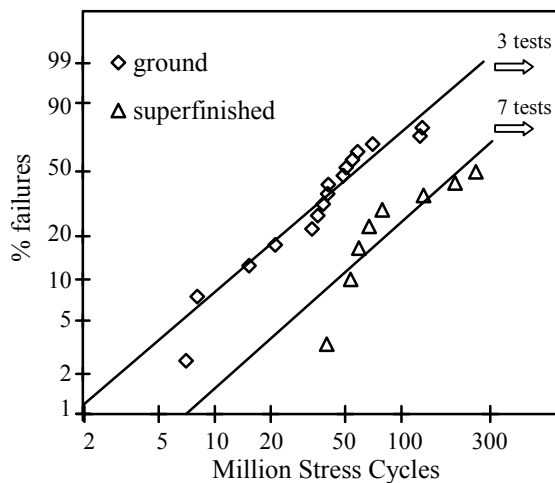


Figure 3: Results of micropitting fatigue tests on ground and superfinished gears.

### 3.0 SCUFFING

Scuffing is a serious form of surface failure that can affect gears running at high speeds or at high temperatures. Although there is no accepted explanation for the mechanism of scuffing, in many situations it is linked to physical failure of the EHL mechanism. To avoid scuffing problems gear designers often specify chemically active extreme pressure (EP) additives in the lubricating oil, some form of surface treatment for the gears such as case-carburising/hardening, nitriding or coatings, or a combination of these. Two particularly promising methods for upgrading the scuffing resistance of steel gears are: improvement of surface finish; and use of super hard coatings, e.g. diamond-like carbon (DLC) coatings. Polishing hardened and ground steel discs can produce a significant improvement in scuffing performance [20]. Superfinished discs used in scuffing tests showed a two fold load limit increase in comparison with ground disks, with the additional benefit of significantly lower friction and bulk metal temperatures. It should be emphasised that the ground and superfinished discs were of the same steel which was case-carburised and hardened to the same specification for both types of finish. The quality of the polishing process used to achieve these results is illustrated in Figure 4, and Figure 5 shows collected results from the series of tests. The lubricant in all tests reported in this paper was Mobiljet 2 at a feed temperature of 100°C.

Thin hard coatings have been found to offer benefits in many non-gearing applications in terms of wear resistance, chemical inertness and low coefficient of sliding friction. They are deposited using different variations of the physical vapour deposition technique using magnetron sputtering [21]. The DLC types have been selected for a number of industrial applications both for tooling and machine elements. Part of this same family are the metal doped DLC coatings (Me-DLC), which appear to offer a better adherence and greater toughness than bare DLC coatings and show particular promise as coatings for gears. A second

type of coating that has been considered is boron carbide ( $B_4C$ ) which is an attractive alternative to Me-DLC, as outlined by Eckardt *et al.* [22], giving enhanced chemical and thermal stability combined with extreme hardness. Moreover, the coating process requires a less reactive gas, which is advantageous. The chemical structure of the coating is amorphous with a majority of  $B_4C$  carbides. Some boron oxides as well as boron oxy-carbides are also normally present with about 15-18 % oxygen located mostly at the surface [23].



Figure 4: A superfinished steel test disc showing high quality finish achieved.

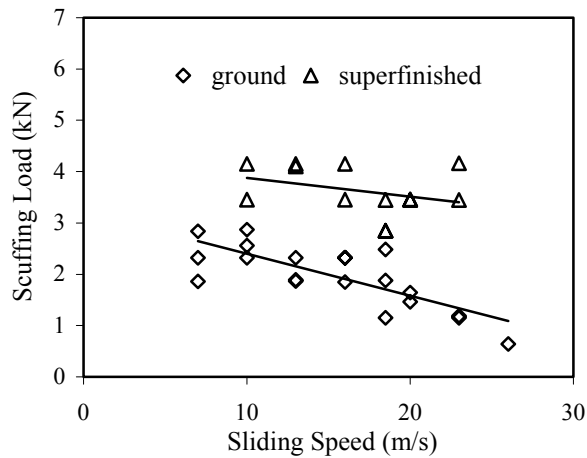


Figure 5: Results of scuffing tests on ground and superfinished discs.

Me-DLC and  $B_4C$  coatings, whose details are given in Table 1, were used in scuffing tests carried out at sliding speeds ranging from 7 m/s to 20 m/s. The tests demonstrate the potential benefits of these coatings on both case-carburised and nitrided steels, although superfinishing achieved a similar performance in terms of scuffing load capacity as may be seen in Figure 6 which ranks a wide range of different material and finish combinations (see Table 2) which have been tested as part of an ongoing programme. The triple combination of a nitrided steel substrate plus superfinishing and a diamond-like coating (configuration 9) shows particularly impressive scuffing resistance. The figure also shows the relative performance of the combinations in terms of average mean bulk temperature of the discs just prior to scuffing and the average traction coefficient under the same conditions. Again, superfinishing appears to confer similar benefits in terms of reduced temperature and traction as that obtained from super hard coatings.

## Understanding Scuffing and Micropitting of Gears

**Table 1: Details of scuffing test coatings**

Coating	Thickness	Elastic Modulus	Hardness
Me-DLC	3.2 $\mu\text{m}$	121 GPa	11.4 GPa
B <sub>4</sub> C	2.7 $\mu\text{m}$	180 GPa	17 GPa

**Table 2: Different substrate/finish/coating configurations tested**

Configuration	Substrate	Finish	Coating	No of tests at each sliding speed		
				7 m/s	16 m/s	20 m/s
1*	case-carburised	ground	none (reference)	3	1	1
2**	case-carburised	superfinished	none	-	2	2
3	case-carburised	ground	Me-DLC	3	3	3
4	case-carburised	ground	B <sub>4</sub> C	2	4	3
5	nitrided	ground, compound layer off	none	4	3	3
6	nitrided	ground, compound layer on	none	4	3	3
7	nitrided	superfinished	none	-	3	3
8	nitrided	ground	Me-DLC	-	1	-
9	nitrided	superfinished	Me-DLC	-	3	-

\* one other test was performed at each of the sliding speeds of 10, 13, 18.5 m/s, plus two other tests at 26 m/s.

\*\* two other tests were performed at each of the sliding speeds of 10, 13, 23 m/s, plus three other tests at 18.5 m/s.

Analysis of EHL between typical gear tooth surfaces in contact strongly suggests that eventual scuffing of ground surfaces can be explained by the physical failure of the lubrication mechanism due to sideways leakage of lubricant near the edges of nominal point contacts, and within nominal line contacts due to waviness in the direction transverse to that of rolling/sliding. Figure 7 shows a scuffing scar on an elliptical contact in a disc machine test. It is possible to envisage the leakage of oil from the loaded area in a transverse direction along the relatively deep valleys between asperities produced by the grinding process as a lubrication failure mechanism. It is interesting to note that for rough ground disc tests, scuffing was initiated at the edges of the contact without exception, and not near the contact centreline where pressures and “flash temperature” are highest. Roughness valleys are therefore seen as vulnerable features of the surface when considering lubrication effects. This concept has been pursued theoretically [24] in a simple model of EHL film failure in which a dry contact analysis was used to provide the geometry of gaps (due to valley features of roughness) between lubricated surfaces under thin film conditions. The magnitude of the transverse pressure gradients needed to cause significant sideways

leakage in these gaps, and hence collapse of the film, is consistent with that present at the edges of real EHL contacts under similar operating conditions. These ideas are being explored more fully with the aid of detailed micro EHL solutions that include these side leakage effects, as discussed in section 4.

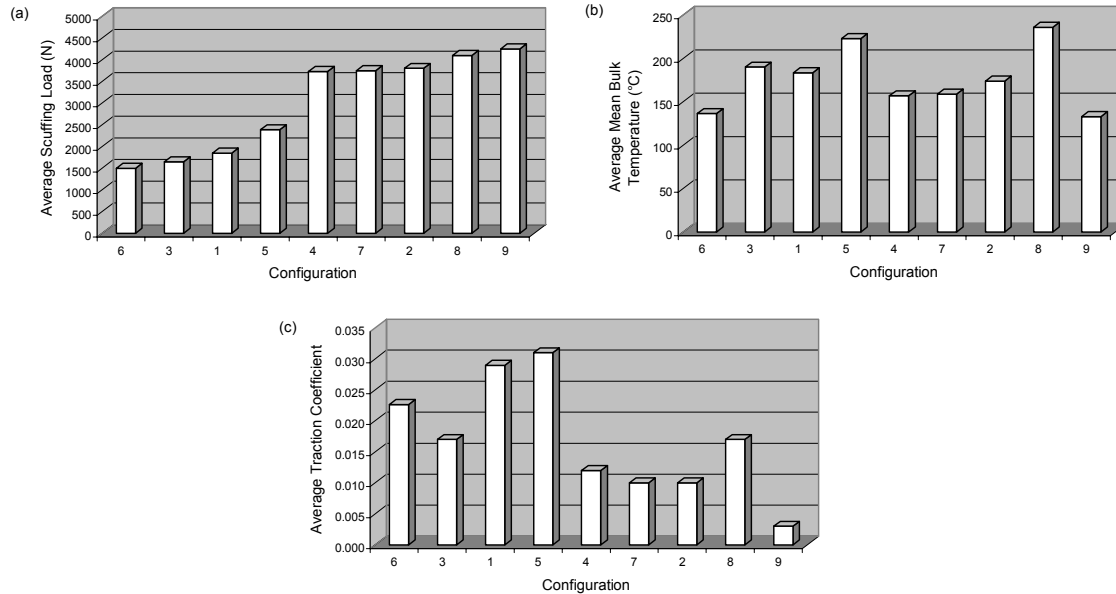


**Figure 6 Comparison of performance between the different configurations (defined in Table 2) for tests performed at 16 m/s sliding speed. Uncoated configurations added for comparison. (a) scuffing load; (b) average mean bulk temperature at scuffing load; (c) average traction coefficient at scuffing load.**

#### 4.0 MICRO EHL THEORY AND APPLICATION TO MICROPITTING

Considerable progress has been made with modelling of roughness in EHL contacts starting with idealised single features or sinusoidal waves and progressing to measured (real) roughness on both line and point contacts. Most analyses are based on a two-dimensional or nominal line contact model. This is a reasonable assumption in the case of conventional involute, parallel axis gears where rolling/sliding takes place across the finishing marks which are close to being two-dimensional, as may be judged from Figure 2.

The early attempts to model micro EHL were based upon a sinusoidal representation of roughness under steady state conditions (Goglia et al [25]; Lubrecht et al [26]; Kweh et al [27]; Elsharkawy and Hamrock [28]) More recently real surfaces as represented by profilometer traces of actual surfaces have been used in steady-state solutions (Sadeghi [29]; Kweh et al [30]; Venner, et al [31]). The problem of non-steady (i.e. moving roughness) conditions has been addressed by Chang and Webster [32], Chang [33], and Chang et al [34] using sinusoidal roughness, and by Ai and Cheng [35] with random roughness. The important influence of non-Newtonian (shear thinning) effects in micro EHL solutions has been reviewed and studied by Chang and Zhao [36]. The inclusion of non-Newtonian lubricant behaviour and consideration of the roughness moving relative to the contact tend to reduce the pressure ripples but also tend to give thinner oil films.

Zhu and co-workers [37,38] were among the first to develop a “mixed” lubrication EHL model for elliptical contacts in which films below an arbitrary low value are regarded as creating contacts with a corresponding simplifying modification of the Reynolds equation presumed at the contacting areas. Their

## Understanding Scuffing and Micropitting of Gears

analyses have predicted a considerable degree of direct surface contact [39], which is stated to be insensitive to the (small) film level at which contact is taken to occur. The treatment of contact in this model is somewhat arbitrary however, and the assumptions made in dealing with contact remain to be verified. In contrast our contribution to rough surface EHL under severe thin film conditions is based on a theoretical model for line contacts (the appropriate configuration for spur gears) that solves the elastic and hydrodynamic film thickness equations simultaneously using a consistent, mass-conserving, fully coupled method [40, 41]. This new robust numerical technique has enabled results to be obtained for extremely low  $\lambda$  values with contact, if it occurs, established directly from solution of the time-dependent equations. A second important feature that emerges using this approach, dependent upon the oil rheology model, is that of lubricant cavitation under severe conditions of thin films/high roughness [42].

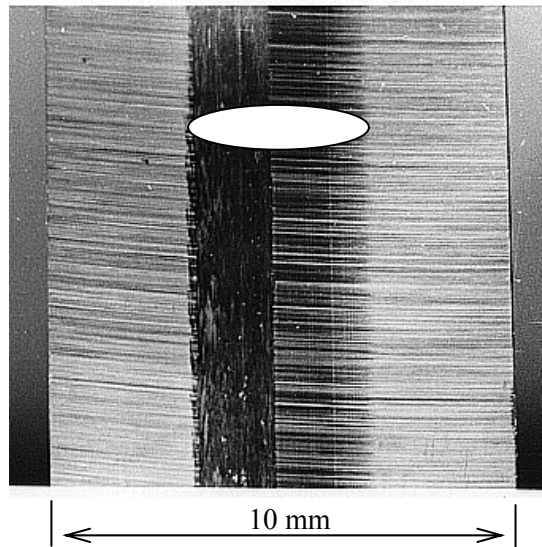


**Figure 7: Scuffing scar on an axially-finished test disc. Superimposed ellipse indicates approximate equivalent Hertzian contact.**

In some circumstances contact occurs between the surfaces as part of the solution process. If, in a particular timestep a converged result is obtained with a negative calculated film thickness, then the most negative film thickness is set to zero. The hydrodynamic equation at this nodal point is deleted from the problem matrix, but the elastic deflection equation is retained. (In this way the film thickness value of zero is a boundary condition for the elastic deflection equation which ensures that the pressure distribution obtained remains entirely consistent with the film shape. The pressure developed in the coupled solution at the contacting node is then an automatic boundary condition for the hydrodynamic equation on both sides of the contacting node.) The timestep is then re-calculated. This procedure is repeated for the timestep, adding no more than one contact point per timestep re-calculation, until a converged result with no negative calculated film thicknesses is obtained. Contact, as calculated in this way, is found to be a relatively infrequent event in the line contact results obtained as discussed below.

A further instance where a full film solution is not obtained at each node point is when what may be termed “in-contact cavitation” occurs. Cavitation at the exit of a contact, where the calculated pressure falls to sub-ambient values, is a natural part of any EHL solution. Situations occur in rough EHL contacts where composite valley features are increasing in volume with time. If flow into such a feature from the micro contacts at either side is insufficient, then the pressure in the composite valley feature will fall. If this effect is sufficiently strong then the oil ‘trapped’ in the composite valley can become entirely decompressed, returning progressively to ambient pressure. When the calculated pressure becomes negative the lubricant is regarded as cavitated. In these solutions the occurrence of in-contact cavitation is found to



increase with the degree of sliding and this suggests, perhaps, a possible erosion wear mechanism that may be related to micropitting damage.

Both localised contact and in-contact cavitation are effects determined from the numerical analysis. The sensitivity of these calculated events to the details of the numerical scheme is the focus of a current investigation by the authors that will be reported in due course. There seems to be little doubt that micro contact does indeed take place between rough surfaces in EHL, as electrical contact resistance measurements provide strong supportive evidence of this phenomenon. The occurrence of calculated in-contact cavitation is a new feature of this kind of analysis, which may be potentially damaging to the surfaces as it takes place in isolation from the ambient atmosphere.

The line contact micro-EHL analysis technique has been applied to a set of profiles corresponding to the later (most heavily loaded) stages in an FZG gear test. The results form part of an investigation programme comparing micropitting performance of test gears using different oils. Use of experimental gear tooth profiles under the real operating conditions of the gears is judged to be an important requirement as surface profile topography is significantly modified by running-in, and engineering interest must be primarily focussed on the stress and film thickness response actually encountered by the components.

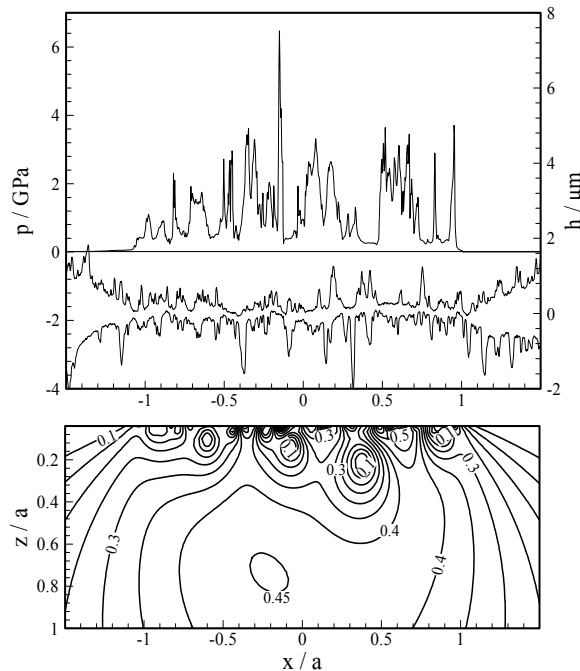


**Figure 8: Pressure and film thickness at a particular timestep in a micro EHL solution for gear tooth contact in an FZG test. Corresponding maximum Hertzian pressure = 1.4 GPa. Also shown are contours of  $\tau$ /GPa, the sub-surface maximum shear stress.**

Some results from this work are shown as follows. Figure 8 shows the pressure and film thickness variation at a particular timestep corresponding to load stage 9 in a standard FZG test in which the equivalent Hertzian (smooth surface) maximum contact pressure is 1.4 GPa. The profiles used in the simulation are taken from the gears after running at this stage, and the properties of the oil are those for the lubricant used in the tests. The FZG pinion speed was 2250 rpm and oil viscosity (0.028 Pas) was taken to be that at the feed temperature of 60°C. Non-Newtonian lubricant behaviour was modelled according to the Eyring equation. For the result shown in Figure 8 a pressure-dependent Eyring stress given by  $\tau_0 = 0.03p$  was used subject to a minimum  $\tau_0$  value of 10 MPa. Also shown beneath the film thickness

## Understanding Scuffing and Micropitting of Gears

distribution is a contour plot of the subsurface maximum shear stress corresponding to the pressure distribution shown. It is clear that pressures well in excess of the Hertzian values are generated on individual micro asperity contacts. Pressure values in the composite valley areas are much lower, but clearly contribute significantly to the load carrying of the overall EHL film. The elevated values and rapid spatial variation of pressure leads to concentrations of shear stress levels close to the surface. Maximum shear stress values as high as 0.7 GPa occur compared with the smooth surface value of 0.42 GPa. Video sequences made up of such figures enable the variation of pressure and film thickness to be assessed in a qualitative way and are invaluable for developing an understanding of the mechanisms at work as individual asperity features enter the Hertzian contact area and subsequently pass through it, as discussed in [41]. Videos for results such as those presented in this paper are available from the authors on CD by request. Contact between individual asperities and internal cavitation have been observed in such numerical solutions, as discussed above and in [42] where a thinner oil ( $\eta_0 = 0.0048$  Pas,  $\alpha = 11.1$  GPa<sup>-1</sup>) was used for the analysis.

The EHL response of these contacts requires a statistical evaluation of loading severity with parameters obtained by averaging over a sufficiently long transient analysis. Figure 9 shows two such parameters (defined in the *Notation* section) used to compare the EHL response of profiles taken from FZG gear teeth at four different load stages. Parameter  $\Phi(p)$  is the fraction of the Hertzian contact area that has a pressure that exceeds  $p$ . Load stage 6 has the least amount of its contact area subject to extremes of pressure, and load stage 9 has the greatest amount. However all cases tend to the same level of extreme pressure with about 0.25% of the area subject to pressures of 4.5 GPa. The maximum pressures are thus seen to be significant in relation to the hardness of the gear teeth (700 Vickers hardness number) suggesting that surface modification is achieved by plastic deformation under the action of the EHL asperity pressures. The fraction of the contact area subject to pressures between 1 and 2 GPa is seen to rank the profiles according to the applied load, whereas true extremes of pressure may well be governed by surface hardness considerations. Figure 9 also gives the cumulative film thickness distribution for small film thickness values for the four profiles. Parameter  $\Phi(h)$  is the fraction of the Hertzian contact area that has a film thickness that is less than  $h$ . The lowest film values observed are of the order 0.075  $\mu\text{m}$ , and the earlier load stages have a greater tendency towards the lower film values, for example 2% of the contact area for load stage 6 is below 0.15  $\mu\text{m}$ , a figure that reduces to 1% for load stage 9. These results thus suggest that the surface modification (running in) induced at each load stage causes the rough surface to adopt a shape that is more able to generate lubricant films on the micro asperities.

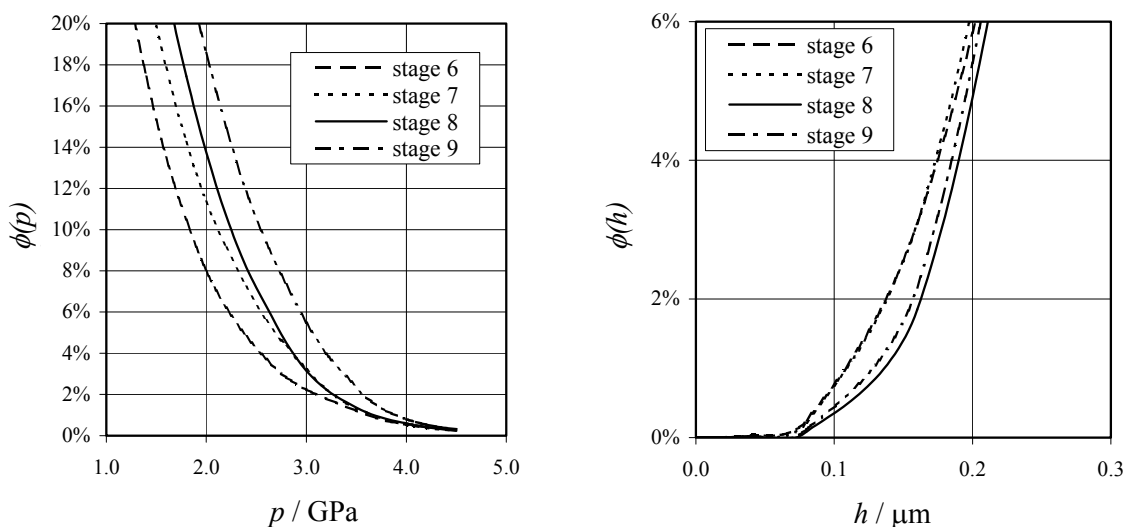


**Figure 9: Maximum pressure  $\Phi(p)$  parameter and low film parameter  $\Phi(h)$  obtained by averaging results of micro EHL solutions corresponding to four different load stages in an FZG gear test.**

The above micro-EHL analyses are based on a line contact model, but in all real gear contacts side-leakage effects will occur even in nominal line contact gears due to edges and waviness of the finish in the axial direction. In gears which are deliberately arranged to have point contacts (such as crowned spur gears, crossed axis gears and special types such as Wildhaber-Novikov) a full side-leakage analysis becomes a necessity. Progress in modelling real roughness on an elliptical contact corresponding to the Cardiff crowned disc machine has been made by Holmes [43]. Figure 10 shows predicted contours of the film under rolling/sliding conditions with roughness of  $R_a = 0.26 \mu\text{m}$  (0.25 mm cut off) on both surfaces. Entrainment is in the direction of the minor axis of the contact. Over most of the contact the behaviour is effectively one-dimensional, but thinning of the film occurs at the transverse edges due to sideways flow of the lubricant in the deep valley features. This thinning (compared to that on the centre line,  $y = 0$ ) is much more severe than that occurring in the corresponding smooth-surface case. This predicted behaviour correlates, qualitatively, with the observation that scuffing in the disc tests initiated at the transverse edges of the contact.

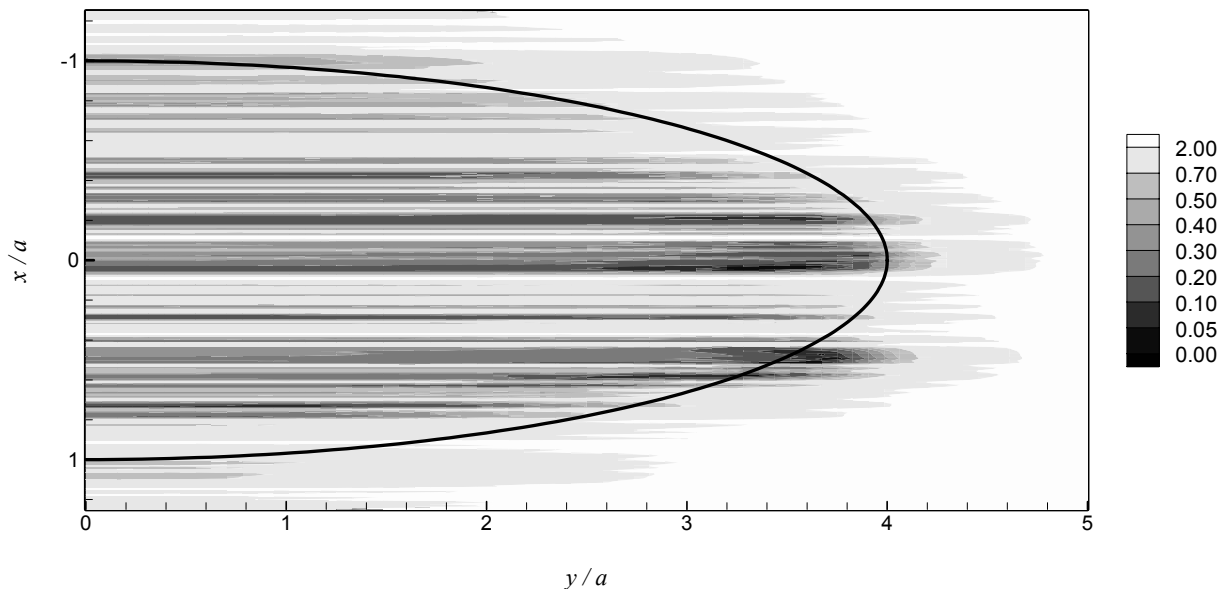


Figure 10: Contours of film thickness/ $\mu\text{m}$  in micro EHL solution corresponding to contact in a crowned disc test as shown in Figure 7. Arrow indicates position of minimum film thickness ( $0.011 \mu\text{m}$ ).

## 5.0 WORM GEARS

The lubricated contacts in worm gears are similar to those occurring in high conformity Wildhaber-Novikov gears [44] giving rise to particularly severe conditions because of the elongated shape of the dry contact region. The contact geometry is non-symmetrical/non-Hertzian and although entrainment of the oil is predominantly along the major axis of the contact its direction varies throughout the area of the conjunction (i.e. a significant spin component of velocity is present). High sliding and heat generation in the contact necessitate a thermal/non-Newtonian EHL treatment. A typical solution obtained for a worm gear contact [45] is shown in Figure 11(a). An interesting feature of the contours shown in this figure is the appearance of a narrow region of almost zero film thickness (within the  $0.47 \mu\text{m}$  contour towards the exit) which effectively separates the overall contact into two regions. This behaviour is explained as follows. A feature of EHL is that within the thin-film main load-bearing part of the contact (corresponding roughly with the equivalent Hertzian region) flow of the lubricant is dominated by the entraining motion of the surfaces (Couette flow). The pressure-induced (Poiseuille) flow is negligible because of the tremendous increase in viscosity due to pressure. Oil entrained into this region will

## Understanding Scuffing and Micropitting of Gears

therefore follow the entrainment streamlines, and these may be determined from purely kinematic considerations of the gears. It also follows that at points where entrainment lines are tangential to the edge of the high pressure region there will be zero net entrainment of oil into the contact at the tangency point, and this indicates a "line" of poor film formation. This hypothesis is reinforced by consideration of Figure 11(b) which shows the entrainment streamlines corresponding to Figure 11(a) together with the dry contact region. The striking similarity between the region of severe film thinning and the path of the tangential entrainment streamline (tangential at point A) within the contact is clear.

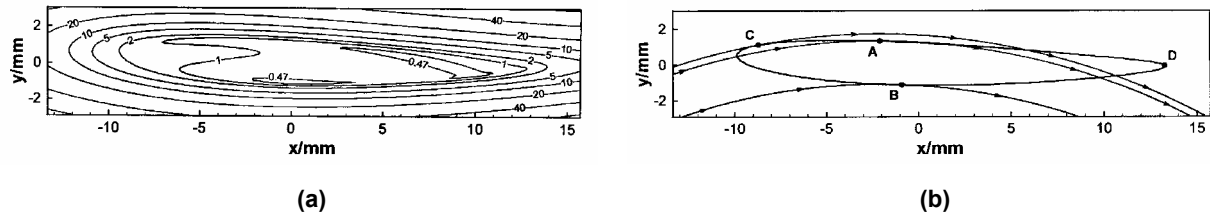


**Figure 11: (a) contours of film thickness/ $\mu\text{m}$  obtained from EHL solution for a worm gear contact (inlet is on the left); (b) corresponding dry elastic contact with key entrainment velocity flowlines superimposed.**

## 6.0 FRICTION

The efficiency of work transfer in a gear mesh is generally in excess of ninety percent, so in many industrial applications overall efficiency of a geared transmission system is not of major concern. However, in high technology applications such as aerospace the losses arising from friction can become of critical importance. For example, the need for ever greater efficiency of propulsion systems for large transport aircraft has led to serious consideration of geared propeller engines or "geared fans" where a reduction gear drive is used to match the speed of an optimum-efficiency gas turbine to that of an efficient propeller or fan. The powers involved are high, typically 30 MW or more. In these applications reduced gear tooth friction can potentially lead to significantly lower amounts of heat being generated at the tooth contacts and hence less bulky cooling arrangements. High gear tooth temperatures are also the predominant factor associated with scuffing, which is a further important reason for reducing friction

Measurements of losses in gearing have been made by Britton et al [46] using a special gearbox mounted on trunnion bearings as illustrated in Figure 12. Power is recirculated between the two pairs of meshing gears which are loaded by means of a torque shaft. After calibrating and deducting the churning and bearing losses, the torque required to drive the rig gives the frictional power at the tooth contacts. Figure 13 shows a comparison of tooth friction losses for both conventionally ground and superfinished gears. This work demonstrates the potential energy-saving benefits of improved surface finish in gearing. Work is now underway to develop theoretical models of gear tooth traction based upon both Eyring and limiting shear stress formulations for the lubricant.

## 7.0 CONCLUSIONS

This brief review of surface distress and elastohydrodynamic lubrication effects in gears demonstrates the importance of the real effects of surface roughness including: non-steady behaviour due to the motion of roughness features relative to the nominal contact; the presence of relatively high degrees of sliding and the consequent frictional heating; non-Hertzian and non-symmetrical geometries. Encouraging progress is being made in the development of new, robust solvers that can deal with the severe conditions of thin films/rough surfaces that characterise real gear tooth contacts. The reality of what has long been called "mixed" lubrication in an otherwise hydrodynamically-lubricated conjunction is beginning to be modelled

and seen in these solutions. A second real feature is that of what we have called “in-contact cavitation” due to the presence of deep valley features within the contact, particularly under sliding conditions. The tendency for micropitting to occur in practice at the beginning and end of the meshing cycle, where sliding is greatest, leads us to suggest cavitation as a possible mechanism for erosive wear that may be part of the micropitting explanation. Edge effects in rough contacts are seen to be of crucial importance in allowing the otherwise stiff and robust EHL mechanism to weaken due to sideways leakage of lubricant. This effect is present in rough contacts to a far greater extent than occurs with perfectly smooth surfaces and reinforces the view that it is strongly related to the real phenomenon of scuffing.

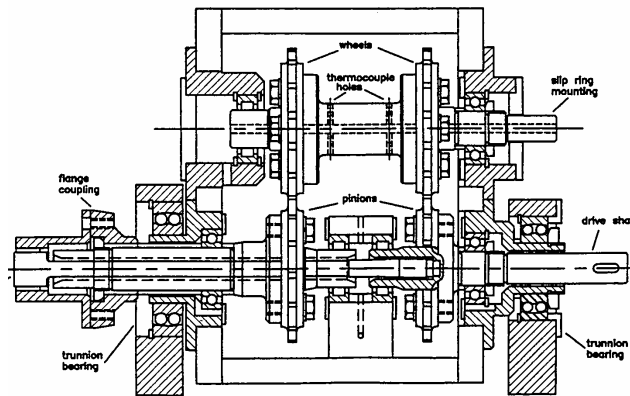


Figure 12: Gear friction rig.

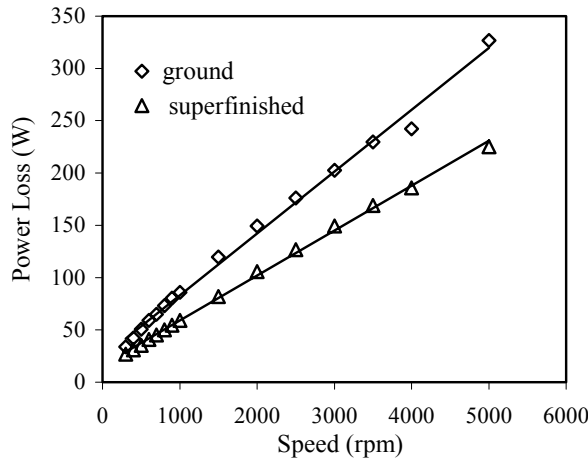


Figure 13: Measured gear mesh friction loss versus speed for ground and superfinished steel gears.

## Understanding Scuffing and Micropitting of Gears

### 8.0 ACKNOWLEDGEMENTS

The authors acknowledge the contribution of Mr C Aylott (Newcastle University) in providing a figure for the paper. Financial support for the research was provided by the British Gear Association, EPSRC and the Ministry of Defence.

### 9.0 NOTATION

$b$	semi-width of Hertzian line contact	m
$E$	elastic modulus	Pa
$E'$	$= 0.5 \left\{ (1 - \nu_1^2) / E_1 + (1 - \nu_2^2) / E_2 \right\}^{-1}$	Pa
$h$	film thickness	m
$h_{min}$	minimum film thickness	Pa
$p$	pressure	Pa
$r_b$	base circle radius	m
$R$	radius of relative curvature of contact	m
$R_1, R_2$	profile radii of teeth at the contact point	m
$s$	distance between contact and pitch point	m
$\bar{u}$	mean entraining speed	m/s
$u_s$	sliding speed	m/s
$w'$	load per unit length of line contact	N/m
$\alpha$	pressure coefficient of viscosity	Pa <sup>-1</sup>
$\eta$	viscosity	Pas
$\eta_0$	viscosity at zero pressure	Pas
$\Lambda$	ratio of film thickness to composite roughness	
$\nu$	Poisson's ratio	
$\sigma$	rms surface roughness	m
$\tau_0$	Eyring shear stress	Pa
$\Phi(h)$	fraction of dry contact area whose film thickness is less than $h$	
$\Phi(p)$	fraction of dry contact area whose pressure exceeds $p$	
$\psi$	pressure angle	rad
$\omega_{1,2}$	Angular velocity of wheel and pinion	rad/s

### 10.0 REFERENCES

- [1] Dowson, D and Higginson, G R, 1966, *Elasto-hydrodynamic Lubrication*, Pergamon Press, Oxford.
- [2] Dyson, A, Naylor, H and Wilson, A R, "The measurement of oil film thickness in elasto-hydrodynamic contacts", Proc. Instn Mech. Engrs Vol 180(3B), 1965, pp 119-134.
- [3] Greenwood, J A and Kauzlarich, J J, "Inlet shear heating in elasto-hydrodynamic lubrication", Trans ASME Jn. Lub. Tech. Vol 95, 1973, pp 417-426.
- [4] Dyson, A, Evans, H P and Snidle, R W 'Wildhaber Novikov circular arc gears: some properties of relevance to their design', Proc. R. Soc., London, A425 (1989), pp. 341-363.
- [5] Chittenden, R J, Dowson, D, Dunn, J F and Taylor, C M, "A theoretical analysis of the isothermal elasto-hydrodynamic lubrication of concentrated contacts", Proc. R. Soc. Lond., Vol A397, 1985, pp 245-269, 271-294.

- [6] ESDU, 1989, "Film thickness in lubricated Hertzian contacts. Part 2: point contacts"
- [7] Harris, T A, *Rolling Bearing Analysis*, Second Edition, Wiley, New York, 1984, p 508.
- [8] O.E.C.D., *Glossary of Terms and Definitions in the Field of Friction, Wear and Lubrication*, 1969, pp 52-53.
- [9] Berthe, D, Flamand, L, Foucher, D and Godet, M, 1980, "Micro-pitting in Hertzian contacts", *Trans ASME, J. Lubr. Tech.*, Vol 102, pp 478-489.
- [10] Olver, A V, Spikes, H A and MacPherson, P B, 1986, "Wear in rolling contacts", *Wear* Vol 112 pp 121-144.
- [11] Zhou, R S, Cheng, H S and Mura, T, 1989, "Micropitting in rolling and sliding contact under mixed lubrication", *Trans ASME, J. of Tribology*, Vol 111, pp 605-613.
- [12] Webster, M N and Norbart, C C J, 1995, "An experimental investigation of micropitting using a roller disk machine", *Tribol. Trans*, Vol 38, pp 883-895.
- [13] Shotter, B A, 1981, "Micropitting, its characteristics and implications, in performance and testing of gear oils and transmission fluids", Institute of Petroleum.
- [14] Webster, M N and Sayles, R S, 1986, "A numerical model for the elastic frictionless contact of real rough surfaces", *Trans ASME, Jn Tribology*, Vol 108, pp 314-320.
- [15] Snidle, R W and Evans, H P, 1994, "A simple method of elastic contact simulation", *Proc. Instn Mech. Engrs Part J Jn of Engng Tribology* Vol 208, pp 291-293.
- [16] Mayeur, C, Sainsot, P and Flamand, L, 1995, "A numerical elastoplastic model for rough contact", *Trans ASME, J. of Tribology*, Vol 117, pp 422-429.
- [17] Kapoor, A and Johnson, K L, 1995, "Plastic ratchetting as a mechanism of erosive wear", *Wear* Vol 190, pp 86-91.
- [18] Tyfour, W R and Beynon, J H, 1994, "The effect of rolling direction reversal on fatigue crack morphology and propagation", *Tribology International*, Vol 27, pp 273-282.
- [19] Krantz, T L, Alanou, M P, Evans, H P and Snidle, R W, "Surface fatigue lives of case-carburized gears with an improved surface finish", *Trans ASME, Journal of Tribology* Vol 123, pp 709-716, 2001.
- [20] Patching, M J, Kweh, C C, Evans, H P and Snidle, R W, 1994, "Conditions for scuffing failure of ground and superfinished steel discs at high sliding speeds using a gas turbine engine oil", *Trans ASME Journal of Tribology* Vol 117, pp 482-489.
- [21] Sproul, W. D., *Physical vapor deposition tool coatings*, *Surface & Coatings Technology*, Vol 81 (1996), pp. 1-7
- [22] Eckardt, T., Bewilogua, K., van der Kolk, G., Hurkmans, T., Trinh, T., Fleischer, W., Improving tribological properties of sputtered boron carbide coatings by process modifications, *Surface and Coatings Technology*, Vol 126 (2000), pp 69-75
- [23] Hu, T., Steihl, L., Rafaniello, W., Fawcett, T., Hawn, D. D., Mashall, J. G., Rozeveld, S. J., Putzig, C. L., Blackson, J. H., Cermignani, W., Robinson, M. G., Structures and properties of disordered boron carbide coatings generated by magnetron sputtering, *Thin Solid Films*, Vol 332 (1998), pp. 80-86
- [24] Evans, H P and Snidle, R W, 1996, "A model for elastohydrodynamic film failure in contacts between rough surfaces having transverse finish", *Trans ASME Journal of Tribology*, Vol 118, pp 847-857.

## Understanding Scuffing and Micropitting of Gears

---

- [25] Goglia, P R, Cusano, C and Conry, T F, 1984, "The effects of surface irregularities on the elastohydrodynamic lubrication of sliding line contacts. Part I - single irregularities; Part II - wavy surfaces", Trans ASME, Jn. of Tribology, Vol. 106, pp 104-112, 113-119.
- [26] Lubrecht, A A, Ten Napel, W E and Bosma, R, 1988, "The influence of longitudinal and transverse roughness on the elastohydrodynamic lubrication of circular contacts", Trans ASME Jn of Tribology, Vol 110, pp 421-426.
- [27] Kweh, C C, Evans, H P, and Snidle, R W, 1989, "Microelastohydrodynamic lubrication of an elliptical contact with transverse and three-dimensional roughness", J. of Tribology, Trans ASME, Vol 111, pp 577-584.
- [28] Elsharkawy, A A and Hamrock, B J, 1991, "Subsurface stresses in micro-EHL line contacts", ASME Journal of Tribology, Vol 113, pp 645-655.
- [29] Sadeghi, F, 1991, "A comparison of the fluid model's effect on the internal stresses of rough surfaces", ASME Journal of Tribology Vol 113, pp 142-149.
- [30] Kweh, C C, Patching, M J, Evans, H P, and Snidle, R W, 1991, "Simulation of elastohydrodynamic contacts between rough surfaces", J. of Tribology, Trans ASME, Paper 91-Trib-36.
- [31] Venner, C H and ten Napel, W E, 1992, "Surface roughness effects in an EHL line contact", ASME Journal of Tribology, Vol 114, pp 616-622.
- [32] Chang, L and Webster, M N, 1991, "A study of elastohydrodynamic lubrication of rough surfaces", ASME Journal of Tribology, Vol 113, pp 110-115.
- [33] Chang, L, 1992, "Traction in thermal elastohydrodynamic lubrication of rough surfaces", ASME journal of Tribology, Vol 114, pp 186-191.
- [34] Chang, L, Webster, M N and Jackson, A, 1993, "On the pressure rippling and roughness deformation in elastohydrodynamic lubrication of rough surfaces", ASME Journal of Tribology, Vol 115, pp 439-444.
- [35] Ai, X and Cheng, H S, 1993, "A transient EHL analysis for line contacts with measured surface roughness using multigrid technique", ASME Journal of Tribology, Paper No 93-Trib-56.
- [36] Chang, L and Zhao, W, 1995, "Fundamental differences between Newtonian and non-Newtonian micro-EHL results", ASME Journal of Tribology, Vol 117, pp 29-35.
- [37] Zhu, D. and Hu, Y Z., 1999, "The study of transition from full film elastohydrodynamic to mixed and boundary lubrication" Proc STLE/ASME H.S. Cheng *Tribology Surveillance*, 150-156.
- [38] Hu, Y Z, and Zhu, D., 2000, "A full numerical solution to the mixed lubrication in point contacts," ASME Journal of Tribology, Vol 122, 1-9.
- [39] Zhu, D. and Hu, Y Z., 2000, "Effects of rough surface topography and orientation on the EHD and mixed lubrication characteristics" Proceedings International Tribology Conference, Nagasaki, 625-630.
- [40] Hughes, T.G., Elcoate, C.D. & Evans, H.P. Coupled solution of the Elastohydrodynamic line contact problem using a differential deflection method. Proc. Instn Mech. Engrs Part C Jn of Mechanical Engineering Science, Vol 214, pp 585 598, 2000.
- [41] Elcoate, C D, Hughes, T G, Evans, H P., and Snidle, R W., 2001, "Transient elastohydrodynamic analysis using a novel coupled differential deflection method" Proc. Instn. Mech. Engrs Part J, Jn of Engng Tribology , Vol 215, pp 319-337.
- [42] Tao, J, Hughes, T G, Evans, H P, & Snidle, R W., 2002, "Elastohydrodynamic response of transverse ground gear teeth". To appear Proc. 28th Leeds-Lyon Symp. on tribology, Elsevier, Amsterdam.



- [43] Holmes, M.J. *Transient analysis of the point contact elastohydrodynamic lubrication problem using coupled solution methods*. PhD thesis, University of Wales, 2002.
- [44] Evans, H P and Snidle, R W, 'Wildhaber-Novikov circular arc gears: Elastohydrodynamics', *Trans ASME Jn of Tribology*, Vol 115, pp 487-492, 1993.
- [45] Sharif, K, Kong, S, Evans, H P and Snidle, R W, "Contact and elastohydrodynamic analysis of worm gears: Part 2, results", *Proc. Instn Mech. Engrs, Part C: Journal of Mechanical Engineering Science* Vol 215 (2001), pp 831-846.
- [46] Britton, R D, Elcoate, C D, Alanou, M P, Evans, H P and Snidle, R W, "Effect of surface finish on gear tooth friction", *Trans ASME Jn. of Tribology*, Vol 122, pp 354-360, 2000.

**Understanding Scuffing and Micropitting of Gears**

---

